

FAR-INFRARED ISO LIMITS ON DUST DISKS AROUND MILLISECOND PULSARS

T. J. W. Lazio¹, J. Fischer¹, and R. S. Foster^{1,2}

¹Naval Research Laboratory, Code 7213, Remote Sensing Division, Washington, DC 20375-5351 USA

²Present address: Booz-Allen & Hamilton Inc., 8283 Greensboro Drive, McLean, VA 22102-3838 USA

ABSTRACT

We report 60 and 90 μm observations of 7 millisecond pulsars with the ISOPHOT instrument and describe our analysis procedures. No pulsars were detected, and typical (3σ) upper limits are 150 mJy. We combine our results with others in the literature and use them to place constraints on the existence of protoplanetary or dust disks around millisecond pulsars.

Key words: Accretion, accretion disks – planetary systems: protoplanetary disks – pulsars: general

1. INTRODUCTION

The first extrasolar planets discovered were found around the millisecond pulsar PSR B1257+12 (Wolszczan & Frail 1992). Various mechanisms have been proposed for their formation (Phinney & Hansen 1992), but all generally rely on an accretion disk around the pulsar within which the planets form. Millisecond pulsars themselves are understood to be neutron stars that have been “spun-up” by the accretion of matter from a companion (van den Heuvel 1995).

Both of these arguments suggest that dust disks may exist around millisecond pulsars. These dust disks may exist regardless of whether or not the pulsar is orbited by planets. The planetary formation process is unlikely to be 100% efficient, and a dust disk may represent the remnant debris from the formation of the planetary system. Alternately, not all accretion disks may give rise to planetary systems, and a dust disk would represent the remnant of the initial accretion that spun-up the pulsar.

A modest number of unsuccessful searches for infrared emission from dust around millisecond pulsars have been conducted. Figure 1 compares the current observational limits for PSR B1257+12 with the predicted emission levels from a dust disk model. The limits for other pulsars are similar. Figure 1 illustrates the need for far-infrared observations.

2. OBSERVATIONS

In order to generate a millisecond pulsar ISOPHOT target list, we compiled a list of millisecond pulsars known

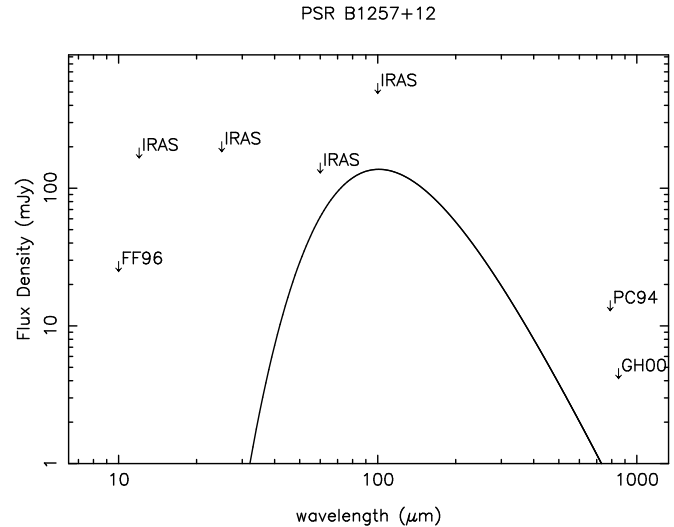


Figure 1. Upper limits on the infrared and sub-millimeter emission from PSR B1257+12. Limits are from Foster & Fischer (1996, FF96 and IRAS), Phillips & Chandler (1994, PC94), and Greaves & Holland (2000, GH00). The solid line shows the expected emission from a $300 M_{\oplus}$ dust disk composed of dust particles $0.1 \mu\text{m}$ in size and heated by 1% of the spin-down luminosity of the pulsar (Foster & Fischer 1996). The pulsar is assumed to be at a distance of 620 pc.

prior to 1994 August and with distances less than 1 kpc. Distances are estimated from the Taylor & Cordes 1993 model and should be accurate to approximately 25%. Most of these millisecond pulsars lie at high Galactic latitudes.

Of these, seven were observed with the ISOPHOT instrument (Lemke et al. 1996) onboard the ISO satellite (Kessler et al. 1996). Table 1 summarizes the observing details. All of the observations used the P32 observing mode with the C100 detector. In this mode the spacecraft was commanded to cover a series of raster pointings around the nominal pulsar position. At each raster pointing an internal chopper pointed the beam toward 13 adjacent sky positions. The throw of the chopper was larger than the offset between raster pointings. The result was that, in general, an individual sky position within the raster was observed multiple times or oversampled. Before and after

each observation of a pulsar, an internal calibration source was observed.

Table 1. Pulsars Observed

Name PSR	λ (μm)	D (pc)	L_{sd} (L_{\odot})	P32 Raster	Time (s)
J0034–0534	90	1000	10	3×8	1402
J1640+2224	60	1190	0.88	3×6	1012
	90	1190	0.88	3×8	848
J1730–2304	60	510	< 0.35	3×6	1590
	90	510	< 0.35	3×8	1232
B1855+09	60	900	1.1	3×6	1012
J2124–3358	60	240	1.7	3×6	1012
	90	240	1.7	3×8	848
J2145–0750	60	500	< 0.048	3×6	1590
	90	500	< 0.048	3×8	848
J2322+2057	60	780	0.62	3×6	1804
	90	780	0.62	3×8	1402

The analysis of the pulsar observations largely followed the standard ISOPHOT analysis. The key difference was the amount of “deglitching” performed. Glitches result from cosmic rays striking the detector or secondary electrons produced by spacecraft materials struck by primary cosmic rays. Failure to remove glitches can corrupt the responsivity drift correction of *all* data, not just those containing the glitches themselves. The standard ISOPHOT analysis pipeline removes glitches but does so without making use of the redundancy implicit in the oversampled P32 observations.

Deglitching proceeded in the following fashion. Within each spacecraft pointing the chopper would sweep past a particular sky position multiple times (typically 3–5 times). For each sky position, the median signal level was determined, then subtracted from all observations at that sky position. The observations from all sky positions were then combined to form a signal strength histogram. A signal strength threshold was specified, and signals above this level were eliminated. Typically 3%–10% of the signals were eliminated in this stage. Depending upon the number of chopper sweeps per spacecraft pointing and deglitching prior to this stage, the median signal strength per sky position could not always be determined accurately. In these cases, additional manual deglitching was done to remove any remaining outlier signals. Our use of the observations of the internal calibration sources followed the standard ISOPHOT analysis pipeline.

After deglitching and calibration using the internal calibration sources, mapping was done within the ISOPHOT Interactive Analysis package. Measurements from the individual detector pixels were co-added to form a sky image,

with the contributions from the individual detector pixels weighted by their distances from the image pixels. Doing so takes into account the beam profile falling on each detector pixel. We also employed a median flat field, which has the effect of reducing substantially our sensitivity to any extended emission in the field but increasing our sensitivity to point sources, as desired for this program.

As an example of the resulting images produced, Figure 2 shows the image of PSR B1855+09. In no case have we identified a point source at the location of a pulsar. Utilizing the inner quarter of the image, we determined the rms noise level. We take our upper limits to be 3 times this rms noise level. Typical (1σ) values are 50 mJy, with higher values seen for pulsars close to the Galactic plane.

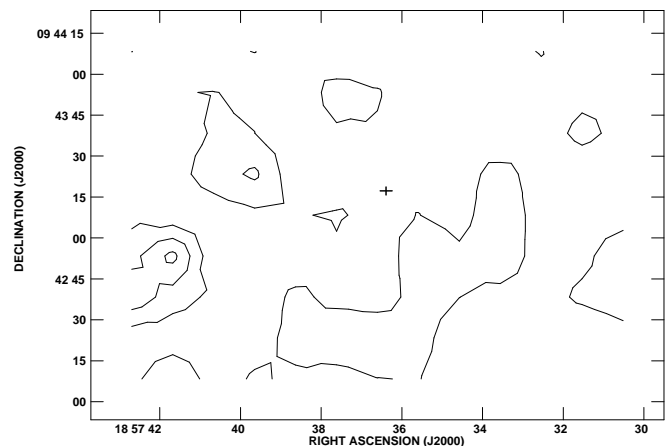


Figure 2. PSR B1855+09 at $60 \mu\text{m}$. The rms noise level is 50 mJy, and the contour levels are 1.5, 1.6, 1.7, and 1.8 Jy. The cross marks the location of the pulsar, and the size of the cross is 5000 times larger than the uncertainty in the pulsar’s location and proper motion.

3. RESULTS

Foster & Fischer (1996) developed a model for the infrared emission from a dust disk around a millisecond pulsar. Their model assumes that the disk consists of particles of a uniform radius a heated by a fraction f_{sd} of the pulsar’s spin-down luminosity L_{sd} . The total mass of the disk is m_d . While the model is simplistic—an actual dust disk presumably consists of particles with a range of sizes, the heating mechanism is left unspecified, and non-equilibrium effects such as stochastic heating are ignored—we believe that this simplicity is justified given the uncertainties of the heating mechanism and of the environs of a millisecond pulsar.

For $f_{\text{sd}} \sim 1\%$, typical dust temperatures are predicted to be $T \approx 10\text{--}50$ K for disks having $m_d \sim 100 M_{\oplus}$ and $a \sim 1 \mu\text{m}$ and illuminated by a pulsar with $L_{\text{sd}} \sim 1 L_{\odot}$. These

temperatures are considerably lower than those assumed ($T \approx 150$ K) by Phillips & Chandler (1994), who estimated disk temperatures by scaling from observations of T Tauri stars. The lower temperatures result from our assumption of a weaker coupling between the pulsar’s spin-down luminosity and the disk. Phillips & Chandler (1994) considered disk temperature to be a major uncertainty in converting from measured flux densities to inferred disk masses. Accordingly, our assumption of a weaker coupling means that larger disk masses can be tolerated without violating the observational constraints.

In addition to these observations with ISO, other infrared and sub-millimeter observations of millisecond pulsars have been conducted. Those observations most relevant to our sample of millisecond pulsars are those by Foster & Fischer (1996) at $10 \mu\text{m}$ and Greaves & Holland (2000) at $850 \mu\text{m}$. Unfortunately, there is little overlap between these three samples of pulsars. Most of the pulsars that have been observed between 10 and $850 \mu\text{m}$ have been observed at only one or two wavelengths. In general, it is therefore not possible to constrain all three parameters of this model with the existing observations.

We therefore adopt an approach in which we infer limits on two parameters of the Foster & Fischer (1996) model for fiducial values of the third parameter. Elsewhere we shall consider the detailed implications for the well-studied objects from our sample (Lazio et al. 2001). Here, as an example, we consider the millisecond pulsar PSR J0034–0534 (Bailes et al. 1994) which has a probable white dwarf companion, is at a distance of 1 kpc, and has a spin-down luminosity of $10 L_{\odot}$. Greaves & Holland (2000) placed a 2σ limit of 3.7 mJy at $850 \mu\text{m}$, and we place a 2σ limit of 50 mJy at $90 \mu\text{m}$. Figure 3 shows the allowed region of the disk mass-grain size plane given these observational limits and an assumed heating efficiency of $f_{\text{sd}} = 1\%$.

Allowed regions in the m_d - a plane occur for one of two possible reasons. First, the peak of the dust disk emission may appear shortward of $90 \mu\text{m}$, where no constraints exist for this pulsar, with the Rayleigh-Jeans tail of the emission falling below the two measured values. This region is to the lower left in Figure 3. Second, the peak of the emission may appear between $90 \mu\text{m}$ and $850 \mu\text{m}$, but with a magnitude comparable to that measured at $90 \mu\text{m}$ so that the Rayleigh-Jeans tail again does not violate the $850 \mu\text{m}$ limit while the Wien tail of the emission does not violate the $90 \mu\text{m}$ limit. This region is to the lower right in Figure 3. Obviously, a lower value of f_{sd} would produce larger allowed regions in the m_d - a plane.

4. CONCLUSIONS

We have reported 60 and $90 \mu\text{m}$ observations of 7 millisecond pulsars with the ISOPHOT instrument. We have described our analysis procedures, which utilized the standard ISOPHOT Interactive Analysis package but also re-

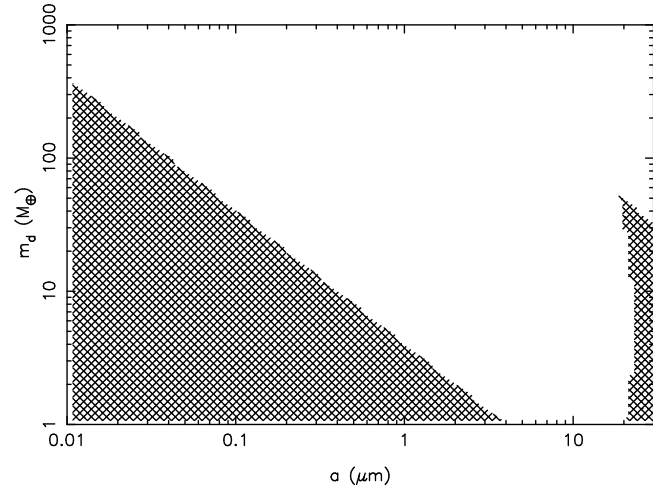


Figure 3. Allowed disk masses and grain sizes for a dust disk orbiting PSR J0034–0534. The cross-hatched region indicates disk masses and grain sizes that do not violate the observational limits at 90 and $850 \mu\text{m}$. A heating efficiency of $f_{\text{sd}} = 1\%$ has been assumed.

lied on considerably more “deglitching” than is usually the case. No pulsars were detected, and typical (3σ) upper limits are 150 mJy.

The current set of pulsars for which mid-infrared, far-infrared, and sub-millimeter observations exists is dominated by pulsars having measurements at only 1 or 2 wavelengths. Measurements at additional wavelengths are required in order to use existing dust disk emission models to place meaningful constraints on the presence or absence of a circumpulsar dust disk.

ACKNOWLEDGEMENTS

We thank the organizers of the ISOPHOT Workshop on PHT32 Oversampled Mapping, particularly R. Tuffs, C. Gabriel, N. Lu, and B. Schulz for their many helpful discussions, and R. Tuffs for his deglitching software. Without their assistance, no results would be reported here. The results reported here are based on observations with ISO, an ESA project with instruments funded by ESA Member States (especially the PI countries: France, Germany, the Netherlands and the United Kingdom) and with the participation of ISAS and NASA. The ISOPHOT data presented in this paper were reduced using PIA, which is a joint development by the ESA Astrophysics Division and the ISOPHOT consortium, with the collaboration of the Infrared Analysis and Processing Center (IPAC) and the Instituto de Astrofísica de Canarias (IAC). This work was supported partially by the NASA ISO grant program. Basic research in astronomy at the NRL is supported by the Office of Naval Research.

REFERENCES

- Bailes, M., et al. 1994, ApJ, 425, L41
- Foster, R. S. & Fischer, J. 1996, ApJ, 460, 902
- Greaves, J. S. & Holland, W. S. 2000, MNRAS, 316, L21
- Kessler, M. F., et al. 1996, A&A, 315, L27

- Lazio, T. J. W., Fischer, J., & Foster, R. S. 2001, ApJ, in preparation
- Lemke, D., et al. 1996, A&A, 315, L64
- Phillips, J. A. & Chandler, C. J. 1994, ApJ, 420, L83
- Phinney, E. S. & Hansen, B. M. S. 1992, in Planets around Pulsars, eds. J. A. Phillips, S. E. Thorsett, & S. R. Kulkarni (San Francisco: ASP) p. 371
- Taylor, J. H. & Cordes, J. M. 1993, ApJ, 411, 674
- van den Heuvel, E. P. J. 1995, J. Astrophys. Astron., 16, 255
- Wolszczan, A. & Frail, D. A. 1992, Nature, 355, 145